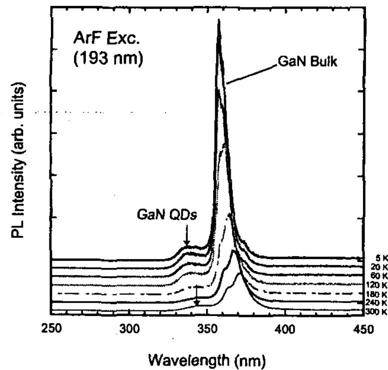

CTuW3 **Fig. 2.** PL spectra from GaN QDs, measured from 5 K to 300 K. The arrows show PL peaks of GaN QDs at 5 and 300 K.

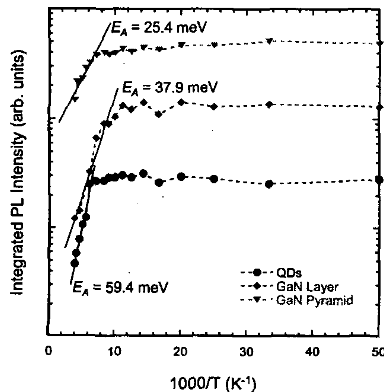

CTuW3 **Fig. 3.** Dependence of integrated PL intensity on temperature.

The intensity of the GaN QD PL peak is smaller than that of the GaN bulk PL peak, because the volume of GaN QDs is much smaller than that of GaN bulk. The two peaks of 363 and 371 nm are observed from GaN bulk at 300 K. The shorter-wavelength peak is from GaN layer under SiO_2, while the longer-wavelength peak is from GaN pyramids, as shown in the previous report.[6]

Figure 3 shows the dependence of integrated PL intensity of GaN QDs, layer under SiO_2, and pyramids in Fig. 2 on temperature. From Fig. 3, the activation energies are estimated to be 59.4, 37.9, and 25.4 meV in GaN QDs, layer under SiO_2, and pyramids, respectively. This result indicates strong confinement of the carriers exists in GaN QDs.

In summary, for the first time, the fabrication and optical properties of selectively-grown GaN QDs are demonstrated. GaN QDs in AlGaN matrix are formed on uniform array of hexagonal GaN pyramids. The PL intensity of GaN QDs is still high at room temperature, which indicates the strong confinement of carriers in GaN QDs.

References

1. S. Tanaka, S. Iwai, and Y. Aoyagi, "Self-assembling GaN quantum dots on $Al_xGa_{1-x}N$ surfaces using a surfactant," Appl. Phys. Lett. 69, 4096–4098 (1996).
2. B. Daudin, F. Widmann, G. Feuillet, Y. Samson, M. Arlery, and J.L. Rouvière, "Stranski-Krastanov growth mode during the molecular beam epitaxy of highly strained GaN," Phys. Rev. B 56, R7069–R7072 (1997).
3. B. Damilano, N. Grandjean, F. Semond, J. Massies, and M. Leroux, "From visible to white light emission by GaN quantum dots on Si (111) substrate," Appl. Phys. Lett. 75, 962–964 (1999).
4. Y. Nagamune, M. Nishioka, S. Tsukamoto, and Y. Arakawa, "GaAs quantum dots with lateral dimension of 25 nm fabricated by selective metalorganic chemical vapor deposition growth," Appl. Phys. Lett. 64, 2495–2497 (1994).
5. K. Tachibana, T. Someya, S. Ishida, and Y. Arakawa, "Selective growth of InGaN quantum dot structures and their microphotoluminescence at room temperature," Appl. Phys. Lett. 76, 3212–3214 (2000).
6. F. Bertram, J. Christen, M. Schmidt, K. Hiramatsu, S. Kitamura, and N. Sawaki, "Direct imaging of local strain relaxation along the {1$\bar{1}$01} side facets and the edges of hexagonal GaN pyramids by cathodoluminescence microscopy," Physica E 2, 552–556 (1998).

CTuW4 **5:30 pm**

Observation of Giant Ambipolar Diffusion Coefficient in Thick InGaN/GaN Multiple-Quantum-Wells

Yin-Chieh Huang, Chi-Kuang Sun, Amber Abare,* Stacia Keller,* Steven P. DenBaars,*
Graduate Institute of Electro-Optical Engineering, National Taiwan University, Taipei, 10617 TAIWAN, R.O.C.; Email: sun@cc.ee.ntu.edu.tw.;
**Department of Electrical and Computer Engineering, University of California, Santa Barbara, CA 93106, USA.*

We report our studies on the 2D lateral diffusion behaviors in InGaN/GaN MQWs using optical techniques. Similar to previous observation of the giant ambipolar diffusion coefficient in GaAs-based n-i-p-i superlattices,[1] we have observed giant ambipolar diffusion coefficient in large well-width InGaN MQWs due to the spatial charge separation by the large built-in piezoelectric field. With a well width of 62Å, a room-temperature ambipolar diffusion coefficient of 2700 ± 500 cm^2/s was measured.

14 periods $In_{0.1}$ GaN/GaN MQWs we studied were grown on a 2.5 μm thick GaN layer. The barrier widths were held at 43Å while the well widths were varied from 12Å to 62Å. The bandgaps of MQWs were between 390–430 nm. TRPL studies on these samples revealed a carrier lifetime between 1–4 ns for short well-width samples (12/25Å) and a much longer lifetime of >35 ns for the large well-width samples (50/62Å), due to the electron/hole wavefunction separation.[2]

The diffusion measurements were performed using standard transmission pump-probe techniques with frequency-doubled UV pulses from a femtosecond Ti:sapphire laser. With a fundamental Gaussian mode, the UV pump pulses excited carriers inside the wells with a Gaussian spatial distribution. Due to well confinement, the photoexcited carriers would diffuse laterally out of the excitation region but would be still confined inside individual wells. Using a delayed probe pulse with the same spot size, its transmission variation would then reflect the carrier density change in the pumping region that was governed by the 2D lateral diffusion. With an equal pump-probe spot size, the initial effective diffusion time constant detected by the probe beam can then be related to the diffusion coefficient D and beam radius w as:

$$\tau_{effective} = \frac{w^2}{4D}. \quad (1)$$

By measuring the diffusion time constant as a function of beam spot size, the values of D can then be obtained.

Figure 1 shows 390 nm room-temperature responses in the 12Å MQW for different beam radii from 4.8 μm to 11μm. The measured initial time constant was found to increase from 150 ps up to 700 ps when the spot size was increased from 4.8 μm up to 11 μm with a square relation, agreeing with equation (1). The time constant was also found to be independent of the laser excitation wavelength and power. Figure 2 plots the measured time constant around time zero vs. pump spot size for the 12Å MQW. A value of 400 ± 100cm^2/s could be obtained for the 2D lateral diffusion coefficient by fitting.

For thick-well samples, drastic time constant

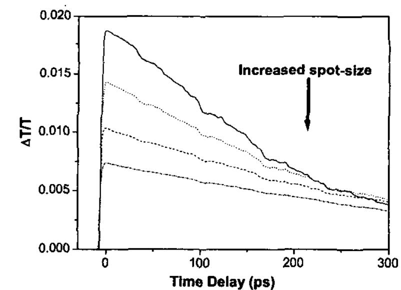

CTuW4 **Fig. 1.** Transient response of the 12Å InGaN/GaN MQW with different spot-sizes. The spot size was increased from 4.8 μm up to 11μm. The laser excitation wavelength was 390 nm.

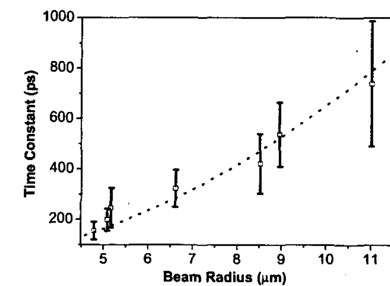

CTuW4 **Fig. 2.** The measured initial diffusion time constant versus pump beam radius for the 12Å well-width sample. The dotted line is a fitting according to equation (1) with a value of D of 400 cm^2/s.

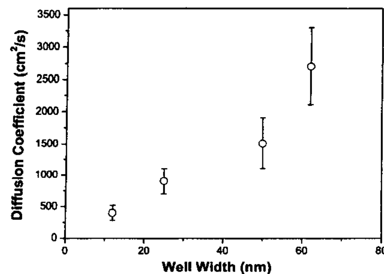

CTuW4 Fig. 3. Measured 2D diffusion coefficient vs. InGaN MQW well-width.

decrease was observed. 2D lateral diffusion coefficient D was found to increase drastically from $400 \pm 100 cm^2/s$ to $2700 \pm 500 cm^2/s$ for well width increased from 12Å up to 62Å shown in Figure 3. This interesting behavior is similar to the "giant ambipolar diffusion constant" observed in GaAs/InGaAs n-i-p-i structures.[1] In thick wells, the fast 2D lateral diffusion was due to spatial separation of the charge carriers of opposite sign which resulted from the strong piezoelectric fields. Due to decomposition of the electron-hole plasma, the attractive Coulomb interaction between electrons and holes was reduced and did no longer compensate the repulsion between carriers of the same type as it did in bulk materials.

References

1. K.H. Gulden, *et al.*, "Giant ambipolar diffusion constant of n-i-p-i doping superlattices," Phys. Rev. Lett. **66**, 373–376 (1991).
2. S.F. Chichibu, *et al.*, "Optical properties of InGaN quantum wells," Mat. Sci. and Eng. B59, 298–306 (1999).

CTuW5 5:45 pm

InGaAsN quantum well structures for long-wavelength lasers

Henning Riechert, *Infineon Technology, Corporate Research Photonics, D-81730 Muenchen, Germany; Email: henning.riechert@infineon.com*

We report on the growth of this material by solid source molecular beam epitaxy (MBE) using an RF-coupled plasma source to generate reactive nitrogen from N_2. Based on optical and structural characterisation we will discuss carrier localisation, nonuniformity in composition, local bonding arrangement as well as the influence of the post-growth annealing treatment commonly used for this material.

Material-related performance data of edge-emitting lasers will be given, along with a comparison of lasers based on InGaAsP and on InGaAsN. For optimised InGaAsN structures, a decrease of single QW transparency current density down to 100 A/cm^2 has been achieved and SQW lasers with threshold current densities as low as 400 A/cm^2 for 1000 μm long, as-cleaved resonators have been made. This represents clearly the lowest laser thresholds reported so far for emission around 1.3 μm from the InGaAsN material system. Based on our results, further potential for material optimisation will be discussed.

Finally, we will present results for InGaAsN-based VCSELs on GaAs, emitting more than 0.5 mW near 1.3 μm in cw operation at 25°C.

CTuW6 6:15 pm

The effect of Mg diffusion on the contact resistance of low doped p-GaN

C.C. Chen, J.L. Yen, and Y.J. Yang, *Department of Electrical Engineering, National Taiwan University, Taipei, Taiwan; Email: yjyang@cc.ee.ntu.edu.tw*

In recent years III-nitride semiconductors have been studied intensively due to its important applications of the short-wavelength optoelectronics and electronics. Although the rapid progress on this material system already makes the commercial laser diodes (LDs) available,[1] still, the critical issue for the device is the lifetime. One of the factors affecting the lifetime is the high p-type contact resistance of the devices, which generates ohmic heating preventing the devices from cw or long-life operation. The obstacles of making a low resistance p-type contact to GaN are mainly in the difficulty to obtain a high in-situ doping level in p-GaN, and the lack of a metal with a large work function to eliminate or reduce the band offset. For the latter issue, various metals and annealing conditions were attempted to reduce the p-type contact and some good results have been achieved.[2] However, for the former issue, the doping levels in p-GaN are mostly limited to the growth systems and techniques used. Besides few reports, the maximum hole concentration in p-GaN is typically $\sim 5 \times 10^{17} cm^{-3}$, which is about two orders of magnitude lower than that of the conventional III-V semiconductors such as GaAs for making a good p-type contact. The post-growth diffusion, which is a conventional way to increase the doping level of as-grown materials, has been unavailable for GaN until recently.[3] In this letter we report for the first time that Mg diffusion was applied to low doped GaN ($\sim 3 \times 10^{16} cm^{-3}$) using Mg_3N_2 as Mg source to reduce the resistance of contact to p-GaN. The results have consistently showed a reduction of contact resistance by ~1.5 orders of magnitude.

A MOCVD grown p-GaN wafer with a hole concentration of $3 \times 10^{16} cm^{-3}$ and a thickness of ~2 μm was used for this study. To conduct the Mg diffusion into p-GaN, the sample was sealed with Ma_3N_2 powder in a vacuumed quartz ampoule and put into a 950°C for 5 min for annealing. Secondary ion mass spectroscopy (SIMS) was used to determine the Mg diffusion profile. Hall measurement was used to characterize the hole concentrations of the sample before and after diffusion. To understand the effect of surface treatment on the contact to p-GaN, the samples were also processed with and without 20 min Aqua regia etching for comparison. A Ni/Au film was deposited on the sample and annealed at 600°C for 1 min to form an ohmic contact. The contact resistance was measured by a transmission line model (TLM) using a linear configuration of $200 \times 80 \mu m^2$ metal pads with spacing varied from 4 to 40 μm linearly in 10 steps.

The measured hole concentration of the p-GaN sample increased from $3 \times 10^{16} cm^{-3}$ to $3 \times 10^{17} cm^{-3}$ after Mg diffusion. Since the diffusion region with the Mg concentration $>5 \times 10^{19} cm^{-3}$ observed from SIMS was only ~0.2 μm thick, based on a ~2 μm thick p-GaN layer, the actual hole concentration near the surface of GaN can be estimated to be $>3 \times 10^{18} cm^{-3}$, which was one order higher than the typical maximum hole concentration obtained from the in-situ doping in crystal growth. Fig. 1 shows the current-voltage (I–V) curves of the Ni/Au contacts to p-GaN wafers under four different process conditions: the as-grown as well as the diffused samples each with and without surface treatment (Aqua regia etching). It clearly indicates that the resistance of the diffused samples was much lower than that of the as-grown samples. There is a turn-on of ~1 V on the I–V curve of the diffused samples without surface etching, indicating the existence of oxide on the GaN surface.[4] With the Aqua regia etching to remove the oxide a linear I-V curve showing an ohmic contact was obtained.

Fig. 2 shows the results of the TLM measurement on the four different wafers same as those used in Fig. 1. The contact resistance was determined to be 2.73 Ω-cm^2 for the as-grown wafer, 6.86×10^{-2} Ω-cm^2 for the as-grown wafer with surface treatment, and 1.93×10^{-3} Ω-cm^2 for the diffused wafer with surface treatment respectively. These results indicate that the contact resistance was reduced by ~1.5 orders of magnitude by the surface etching only,[4] and improved by another ~1.5 orders of magnitude by the Mg diffusion. The improvement from the Mg diffusion can be explained as the following model: Since the transport property of the metal-semiconductor contact is dominated by the tunneling mech-

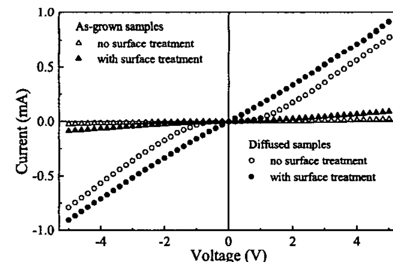

CTuW6 Fig. 1. Current-voltage curves of the samples processed under four different conditions.

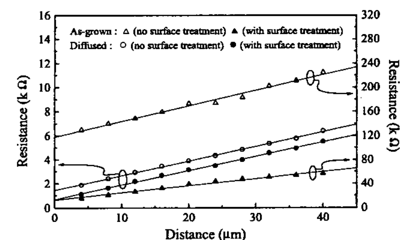

CTuW6 Fig. 2. Contact resistance measured by the transmission line model on the four different samples as same as those used in Fig. 1.